Three-Dimensional Two-Impulsive Orbital Maneuvers with Time Limit

EVANDRO MARCONI ROCCO
ANTONIO FERNANDO BERTACHINI DE ALMEIDA PRADO
MARCELO LOPES DE OLIVEIRA E SOUZA

Instituto Nacional de Pesquisas Espaciais - INPE
C. P. 515, CEP 12227-010 - São José dos Campos, SP, Brazil, fax: (+5512) 3208 6226
E-mail: evandro@dem.inpe.br; prado@dem.inpe.br; marcelo@dem.inpe.br

Abstract: The problem of three-dimensional two-impulsive orbital maneuvers between two elliptical orbits with minimum fuel consumption, but having a time limit, is considered in the present paper. This limit in the time generates a new characteristic to the problem, which eliminates the majority of the methods available in the literature. Equations available in the literature are used and some new ones are developed to consider cases with different geometries. Those equations are then solved and a software is implemented to perform the orbital maneuvers. The original equations are presented in the literature without any numerical results, so, the new cases considered and the solutions and implementation of the method available in the literatures are the contributions shown here. The software was used with success in several different situations.

Key Words: Orbital Maneuvers, Astrodynamics, Impulsive Control.

1 Introduction

The majority of the spacecrafts that have been placed in orbit around the Earth use the basic concepts of orbital transfers. During the launch, the spacecraft is placed in a parking orbit distinct from the final one which it was designed. Therefore, to reach the desired final orbit, the spacecraft must perform orbital transfer maneuvers. Beyond this, the spacecraft orbit must be corrected periodically because there are perturbations acting on it.

There are many alternatives to solve this problem in the literature, considering different assumptions. An important field of solutions considers the low thrust maneuver, where a force with low magnitude is used during a finite time. So, to obtain the trajectory of the spacecraft, the equations of motion must be integrated by numerical algorithms. Some results using this model can be seen in references [1] to [15]. There is also an alternative approach, which uses the concept of an impulsive thrust. This is the situation where the thrust has an infinity magnitude and is applied during a negligible time. Several papers used this approach, like references [16] to [42].

In this work, we consider the problem of two-impulse orbital transfers between non-coplanar elliptical orbits with minimum fuel consumption, but with a time limit for this transfer. This time limit imposes a new characteristic to the problem that rules out the majority of the transfer methods available in the literature. Therefore, the transfer methods must be adapted to this new constraint. The equations presented by Eckel and Vinh [33] are used, but some new equations, to extend the method to cases with different geometry, are developed. Then, the problem is solved and those equations are used to develop a new software for orbital maneuvers.

2 Definition of the Problem

The orbital transfer of a spacecraft from an initial orbit to a desired final orbit consists in a change of state (position, velocity and mass) of the spacecraft, from initial conditions $\vec{r}_0$, $\vec{v}_0$ and m_0 at time t_0 to the final conditions $\vec{r}_f$, $\vec{v}_f$ and m_f at time t_f ($t_f \geq t_0$), as shown in Fig. 1. The maneuver can be classified as: maneuvers partially free, when one or more parameter is free (for example, the time spent by the maneuver); or maneuvers completely constrained, when all the parameters are constrained. In this case the spacecraft performs an orbital transfer maneuver from a specific point in the initial orbit to another specific point in the final orbit (for example, the rendezvous maneuvers). In this work, based in Rocco [40], we consider the orbital transfer maneuvers partially free, and that the spacecraft propulsion system is able to apply an impulsive thrust. Therefore, we have the instantaneous variation of the spacecraft velocity.

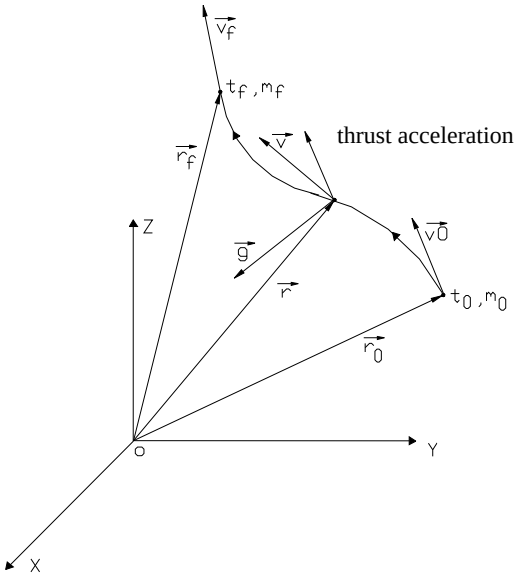

Fig. 1 – Orbital Transfer.

3 Presentation of the Method

The bases for this method are the equations presented by Eckel and Vinh [33] that provides: the transfer orbit between non-coplanar elliptical orbits with minimum fuel and fixed transfer time; or the minimum transfer time for a prescribed fuel consumption. In the present work we consider only the problem with fixed transfer time. The equations were presented in the literature, but the method was not implemented neither tested in Eckel and Vinh [33], and it is valid only for a specific geometry. They used the plane of the transfer orbit as the reference plane but we decided to use the equatorial plane as the reference plane because, in this way, it is easy to obtain and to apply the results in real applications. Using the transfer orbit as the reference plane almost all the results obtained belongs to the same specific geometry, so we changed the reference system, adding the equations 1 to 6 to consider cases with more complex geometry. Thus, this modification, the implementation and the solutions using this method are contributions of this work. After that the method was implemented to develop a software for orbital maneuvers. By varying the time spent in the maneuver, the software developed provides a set of results that are the solutions of the problem of bi-impulsive optimal orbital transfer with time limit.

Given two non-coplanar terminal orbits we desire to obtain a transfer orbit with minimum fuel consumption and fixed time transfer. The orbits are specified by their orbital elements, as shown in Table 1 (subscript 1: initial orbit; subscript 2: final orbit; no subscript: transfer orbit).

Table 1 – Orbital Elements.

a	Semi-major axis
e	Eccentricity
p	Semi-latus rectum
ω	Longitude of the periapsis
i	Inclination
Ω	Right ascension of the ascending node
M	Mean anomaly
E	Eccentric anomaly
λ	Angle between the planes of the initial and final orbits
β_1	True anomaly of the ascending node N obtained in the plane of the initial orbit
β_2	True anomaly of the ascending node N obtained in the plane of the final orbit
I_1	Location of the first impulse
I_2	Location of the second impulse
Δ	Transfer angle obtained in the plane of the transfer orbit
γ_1	Plane change angle resulted from the first impulse
γ_2	Plane change angle resulted from the second impulse
V_1	Velocity increment generated by the first impulse
V_2	Velocity increment generated by the second impulse
V	Total velocity increment
T	Time spent by the maneuver
α_1	True anomaly of the point I_1 obtained in the plane of the initial orbit
α_2	True anomaly of the point I_2 obtained in the plane of the final orbit
r_1	Distance from point I_1
r_2	Distance from point I_2
f_1	True anomaly of the point I_1 obtained in the plane of the transfer orbit
f_2	True anomaly of the point I_2 obtained in the plane of the transfer orbit
x_1	Radial component of the first impulse
x_2	Radial component of the second impulse
y_1	Transverse component of the first impulse in the plane of the initial orbit
y_2	Transverse component of the second impulse in the plane of the transfer orbit
z_1	Component of the first impulse orthogonal of the initial orbit
z_2	Component of the second impulse orthogonal of the transfer orbit
h_i	Horizontal component of V_i

Depending on the intersection of the orbital planes, there are four possible geometries for the maneuvers, as shown in Figs. 2 to 5.

Figure 2 presents the geometry of the maneuver when $\Omega_2 > \Omega_1$ and $i_2 > i_1$. Figure 3 presents the geometry when $\Omega_1 > \Omega_2$ and $i_1 > i_2$.

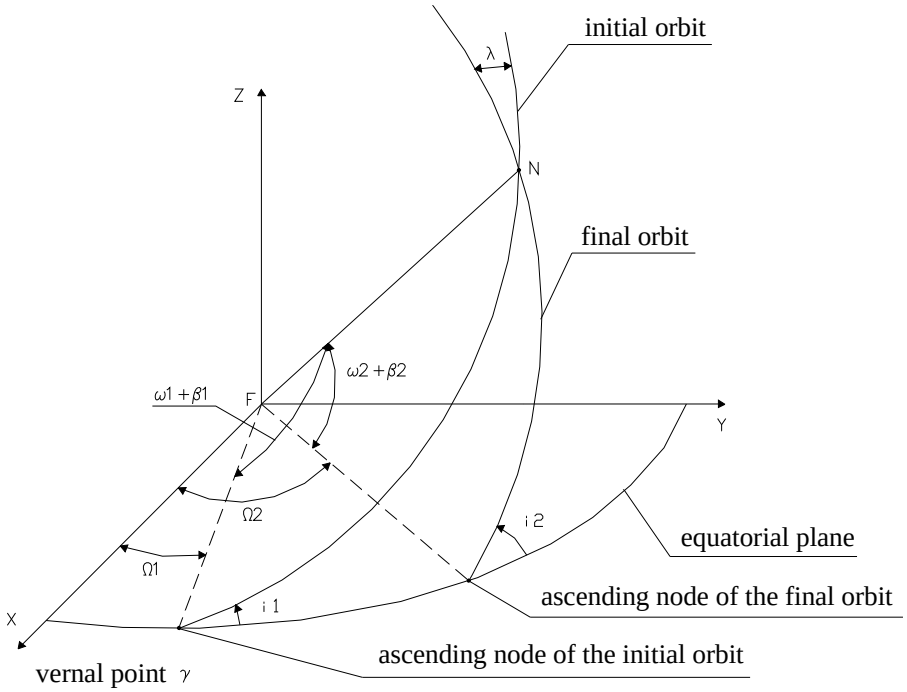

Fig. 2 – Geometry of the Maneuver when $\Omega_2 > \Omega_1$ and $i_2 > i_1$.

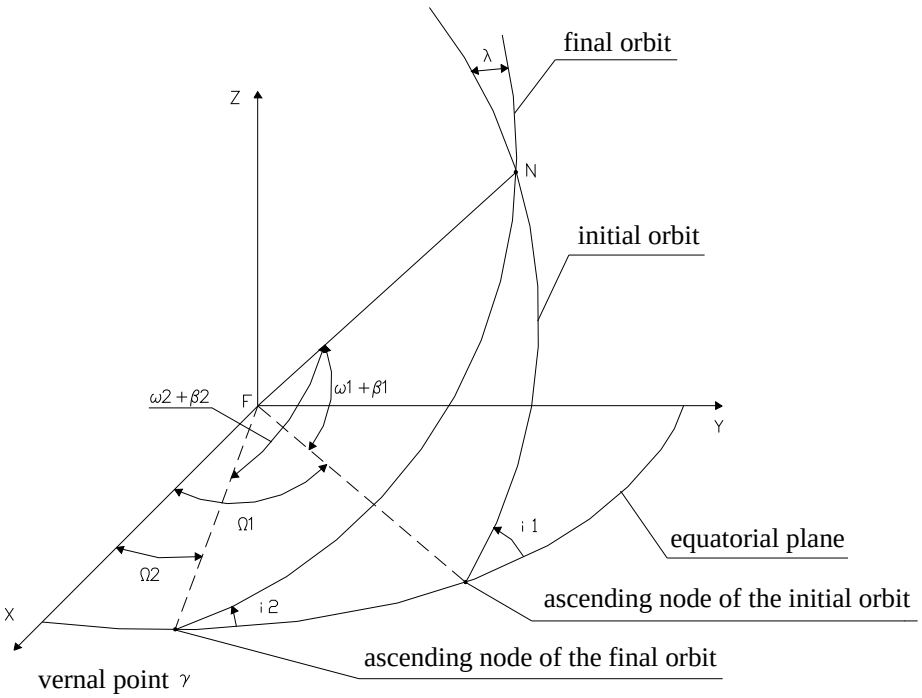

Fig. 3 – Geometry of the Maneuver when $\Omega_1 > \Omega_2$ and $i_1 > i_2$.

Figure 4 presents the geometry of the maneuver when $\Omega_2 > \Omega_1$ and $i_1 > i_2$. Figure 5 presents the geometry when $\Omega_1 > \Omega_2$ and $i_2 > i_1$.

Depending on the locations of the impulses, there are three possible cases (shown in Figs. 6 to 8).

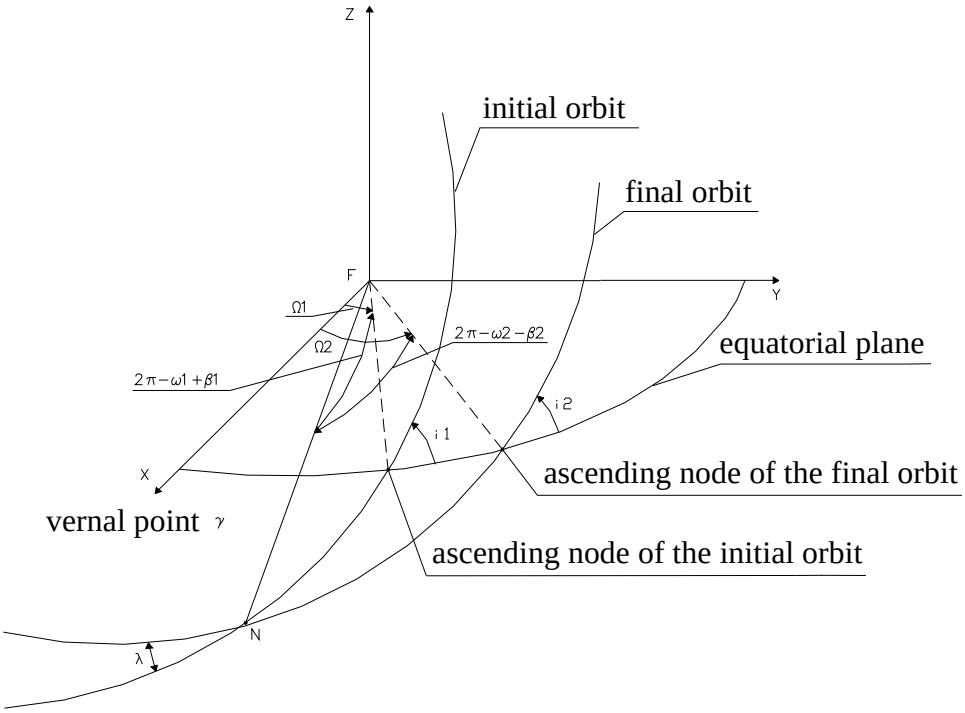

Fig. 4 – Geometry of the maneuver When $\Omega_2 > \Omega_1$ and $i_1 > i_2$.

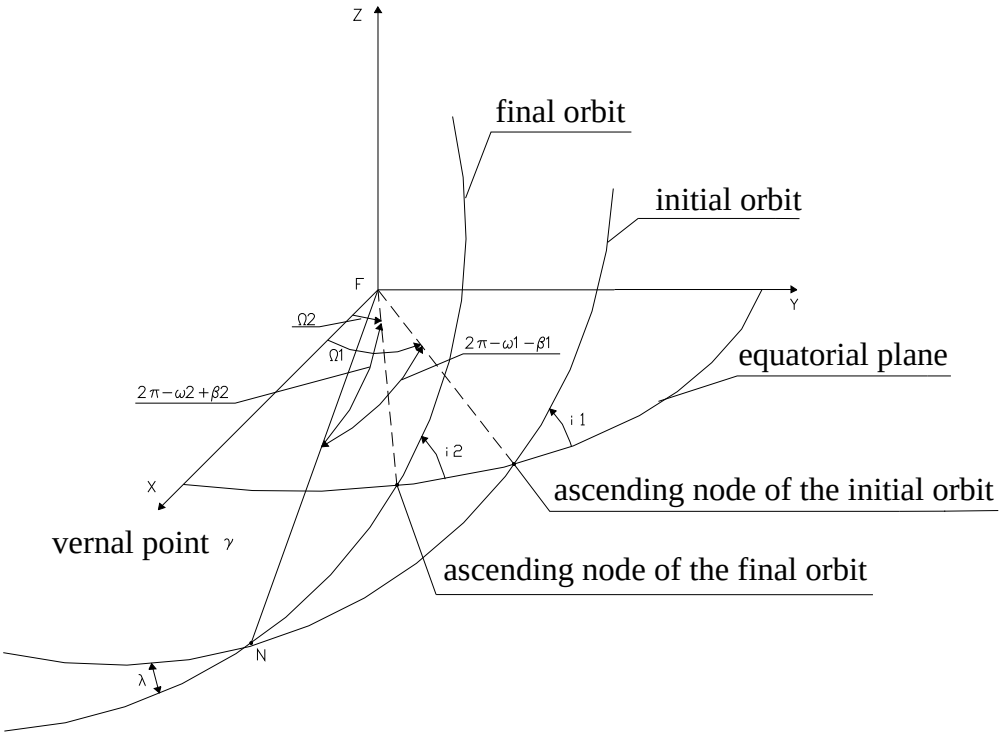

Fig. 5 – Geometry of the maneuver When $\Omega_1 > \Omega_2$ and $i_2 > i_1$.

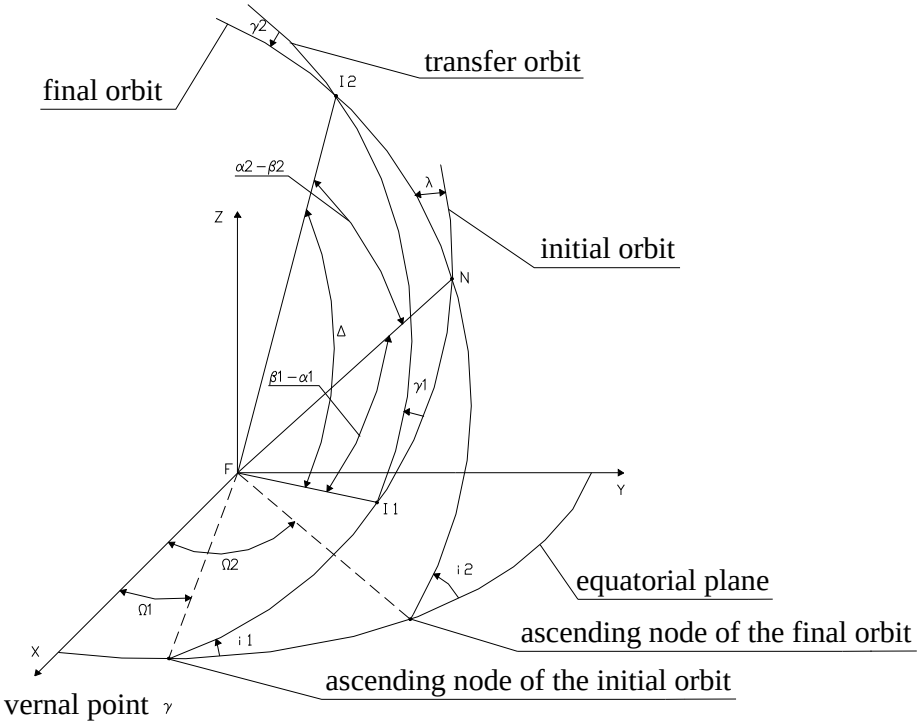

Fig. 6 – Case 1: I_1 before N and I_2 after N.

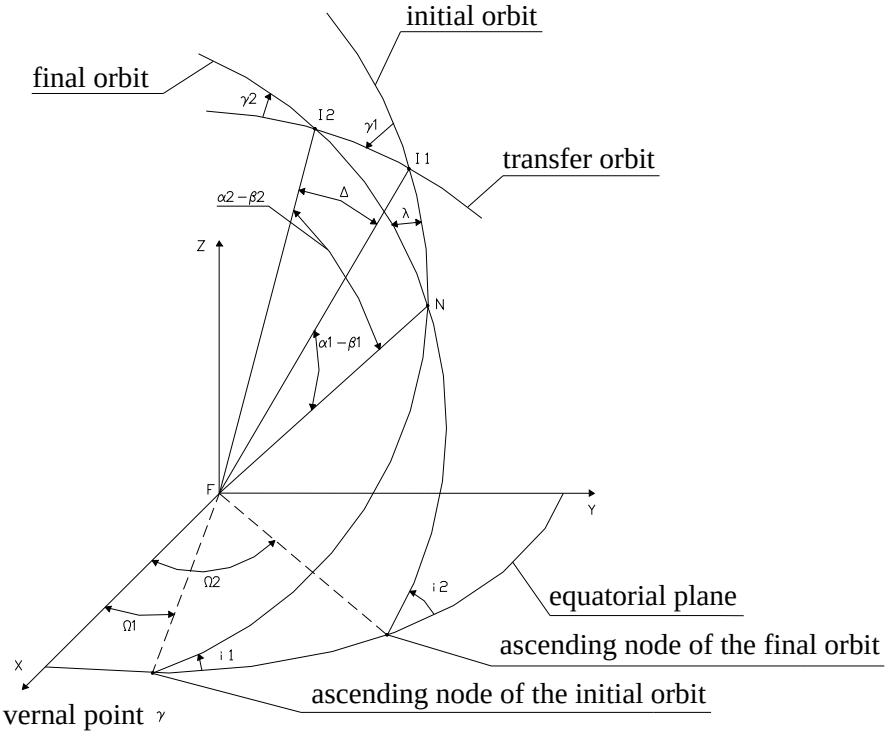

Fig. 7 – Case 2: I_1 and I_2 after N.

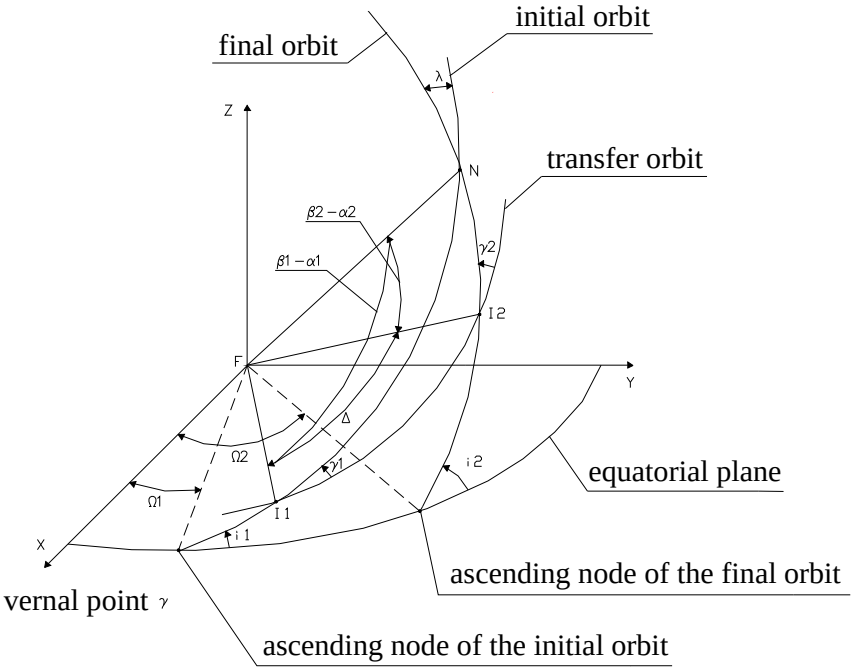

Fig. 8 – Case 3: I_1 and I_2 before N.

Combining these three cases with the four possible geometries for the transfer maneuver, there is a set of twelve cases that can be solved by the software developed. Thus, from the geometry of the maneuver, we obtain β_1, β_2, λ and the transfer angle Δ by [42]:

$$\beta_1 = \arctan\left[\frac{\sin(\Omega_2-\Omega_1)\tan(180^\circ - i_2)}{\sin i_1 + \tan(180^\circ - i_2)\cos i_1 \cos(\Omega_2-\Omega_1)}\right] - \omega_1 \tag{1}$$

$$\beta_2 = \arctan\left[\frac{\sin(\Omega_2-\Omega_1)\tan i_1}{\sin i_2 + \tan i_1 \cos(180^\circ - i_2)\cos(\Omega_2-\Omega_1)}\right] - \omega_2 \tag{2}$$

$$\lambda = \arcsin\left[\frac{\sin(\Omega_2-\Omega_1)\sin i_1}{\sin(\omega_2+\beta 2)}\right] = \arcsin\left[\frac{\sin(\Omega_2-\Omega_1)\sin i_2}{\sin(\omega_1+\beta_1)}\right] \tag{3}$$

$$\cos\Delta = \cos(\beta_1-\alpha_1)\cos(\alpha_2-\beta_2) + \\ + \sin(\beta_1-\alpha_1)\sin(\alpha_2-\beta_2)\cos(180^\circ-\lambda) \tag{4}$$

$$\sin\Delta = \frac{\sin(\alpha_2-\beta_2)\sin(180^\circ-\lambda)}{\sin B} \tag{5}$$

$$B = \arctan\left[\frac{\sin(180^\circ-\lambda)}{\sin(\beta_1-\alpha_1)\cot(\alpha_2-\beta_2) - \cos(\beta_1-\alpha_1)\cos(180^\circ-\lambda)}\right] \tag{6}$$

Considering that the spacecraft propulsion system is able to apply an impulsive thrust and that the maneuver is bi-impulsive, the total velocity increment is:

$$V = V_1 + V_2 = F(\mathrm{X}) \tag{7}$$

where X is an arbitrary variable for the transfer.

The time of the transfer is:

$$T = G(X) \tag{8}$$

Therefore, the problem is the minimization of V for a prescribed T. If the transfer time is prescribed as being equal to a value T_0, we have the constraint relation:

$$T - T_0 = 0 \tag{9}$$

Thus, we have the performance index:

$$J = V + k(T - T_0) \tag{10}$$

From Eckel and Vinh [33], we have that the solution of the problem depends on three variables: the semi-latus rectum p of the transfer orbit and the true anomalies α_1 and α_2 that define the position of impulses in the initial and final orbits. Therefore, we have the necessary conditions:

$$\begin{aligned}\frac{\partial V}{\partial p}+k\frac{\partial \mathrm{T}}{\partial p}&=0\\ \frac{\partial V}{\partial \alpha_1}+k\frac{\partial \mathrm{T}}{\partial \alpha_1}&=0\\ \frac{\partial V}{\partial \alpha_2}+k\frac{\partial \mathrm{T}}{\partial \alpha_2}&=0\end{aligned} \tag{11}$$

By eliminating the Lagrange's multiplier k from equations 11, there is a set of two equations:

$$\begin{aligned}\frac{\partial V}{\partial p}\frac{\partial T}{\partial \alpha_1}-\frac{\partial V}{\partial \alpha_1}\frac{\partial T}{\partial p}&=0\\ \frac{\partial V}{\partial p}\frac{\partial T}{\partial \alpha_2}-\frac{\partial V}{\partial \alpha_2}\frac{\partial T}{\partial p}&=0\end{aligned} \tag{12}$$

Evaluating the partial derivatives in these equations and doing some simplifications, the final optimal conditions are:

$$\begin{aligned}&\left(X_1+YZe\sin f_2\right)\left(S_1q_1-T_1e\sin f_1\right)+S_1T_1+\\ &+W_1\left(\frac{W_1-W_2}{\sin\Delta}q_2-W_1\tan\frac{\Delta}{2}\right)-\frac{W_1Z\,e\,r_1e_1\sin\alpha_1}{q_1p_1\sin f_1\sin\gamma_1}=0\end{aligned} \tag{13}$$

$$\begin{aligned}&\left(X_2+YZe\sin f_1\right)\left(S_2q_2-T_2e\sin f_2\right)+S_2T_2-\\ &-W_2\left(\frac{W_2-W_1}{\sin\Delta}q_1-W_2\tan\frac{\Delta}{2}\right)+\frac{W_2Z\,e\,r_2e_2\sin\alpha_2}{q_2p_2\sin f_2\sin\gamma_2}=0\end{aligned} \tag{14}$$

which use the following relations:

$$r_i=\frac{p_i}{1+e_i\cos\alpha_i} \tag{15}$$

$$f_1=\arctan\left[\cot\Delta-\frac{r_1\left(p-r_2\right)}{r_2\left(p-r_1\right)\sin\Delta}\right] \tag{16}$$

$$f_2=\arctan\left[\frac{r_2\left(p-r_1\right)}{r_1\left(p-r_2\right)\sin\Delta}-\operatorname{cotg}\Delta\right]$$

$$e=\frac{r_2-r_1}{r_1\cos f_1-r_2\cos f_2} \tag{17}$$

$$\gamma_1=\arcsin\left[-\frac{\sin\left(\beta_2-\alpha_2\right)}{\sin\Delta}\sin\phi\right] \tag{18}$$

$$\gamma_2=\arcsin\left[\frac{\sin\left(\beta_1-\alpha_1\right)}{\sin\Delta}\sin\phi\right]$$

$$S_i=\frac{x_i}{V_i} \tag{19}$$

$$T_i=\frac{y_i}{V_i} \tag{20}$$

$$W_i=\frac{z_i}{V_i} \tag{21}$$

$$q_i=\frac{p}{r_i} \tag{22}$$

$$X_1=\frac{S_1\cos\Delta-S_2}{\sin\Delta}+T_1 \tag{23}$$

$$X_2=\frac{S_1-S_2\cos\Delta}{\sin\Delta}+T_2$$

$$\begin{aligned}Y=\frac{1}{\left(1-e^2\right)\sin\Delta}&\left[3e^2\mathrm{T}\sqrt{\frac{\mu}{p^3}}-2e\left(\frac{1}{q_2\sin f_2}\right.\right.\\ &\left.\left.-\frac{1}{q_1\sin f_1}\right)+\operatorname{cotg}f_2-\operatorname{cotg}f_1\right]\end{aligned} \tag{24}$$

$$Z=\frac{q_2X_2-q_1X_1+\left(S_1+S_2\right)\mathrm{tg}\,\Delta/2}{\operatorname{cotg}f_1-\operatorname{cotg}f_2+Y\left[\left(1+e^2\right)\sin\Delta+2e\left(\sin f_2-\sin f_1\right)\right]} \tag{25}$$

The semi-latus rectum, the semi-major axis and the components of the impulses are given by equations 26 to 31. The necessary velocity increment to perform the maneuver can be obtained using equation 32.

$$p=\frac{r_1r_2\left(\cos f_1-\cos f_2\right)}{r_1\cos f_1-r_2\cos f_2} \tag{26}$$

$$a = \frac{p}{1-e^2} \tag{27}$$

$$x_1 = \sqrt{\mu}\left(\frac{e}{\sqrt{p}}\sin f_1 - \frac{e_1}{\sqrt{p_1}}\sin\alpha_1\right) \tag{28}$$

$$x_2 = \sqrt{\mu}\left(\frac{e_2}{\sqrt{p_2}}\sin\alpha_2 - \frac{e}{\sqrt{p}}\sin f_2\right)$$

$$y_1 = \frac{\sqrt{\mu}}{r_1}\left(\sqrt{p} - \sqrt{p_1}\cos\gamma_1\right) \tag{29}$$

$$y_2 = \frac{\sqrt{\mu}}{r_2}\left(\sqrt{p_2}\cos\gamma_2 - \sqrt{p}\right)$$

$$z_i = \frac{\sqrt{\mu p_i}}{r_i}\sin\gamma_i \tag{30}$$

$$h_i = \left(y_i^{\,2} + z_i^{\,2}\right)^{1/2} \tag{31}$$

$$V_i = \left(x_i^{\,2} + h_i^{\,2}\right)^{1/2} \tag{32}$$

The total time spent in the maneuver can be obtained using the following equations:

$$E_i = \arccos\left(\frac{e+\cos f_i}{1+e\cos f_i}\right) \tag{33}$$

$$\sin E_i = \frac{\sqrt{1-e^2}\sin f_i}{1+e\cos f_i} \tag{34}$$

$$M_i = E_i - e\sin E_i \tag{35}$$

$$\mathrm{T} = \sqrt{\frac{a^3}{\mu}}\left(M_{I_2} - M_{I_1} + 2\pi N\right) \tag{36}$$

Therefore, there is an equation system composed by equations 9, 13 and 14. Solving this equation system by the Newton Raphson Method [43] we obtain the transfer orbit that performs the maneuver spending a minimum fuel consumption, but with a specific time.

4- RESULTS

Figures 9 to 26 present some of the results obtained in Rocco [40] and [41] with the software developed. They not show only the tendency of the parameters, but they also quantify the evolution of the variables studied. The graphs were obtained through the variation of the total time spent in the maneuver. Thus, each point was obtained by executing the software with a given time. The points were joined by a line that shows the behaviour of that orbital element.

The first example (Figures 9 to 14, 25 and 26) used here is a maneuver of small amplitude between an initial orbit with semi-major axis of 12030 km, eccentricity 0.02, inclination 0.00873 rad, longitude of the periapse 3.17649 rad, longitude of the ascending node zero and a final orbit with semi-major axis of 11994.7 km, eccentricity 0.016, inclination 0.00602 rad, longitude of the periapse 3.05171 rad, right ascension of the ascending node 0.15568. This maneuver shows that the method applied here is suitable for maneuvers of stationkeeeping. In this example we used as initial values l = 12033.55 km, α_1 = 4.03575149 rad, and α_2 = 5.94012897 rad.

As a second example (Figures 15 to 24), we performed a maneuver between an initial orbit with semi-major axis of 15000 km, eccentricity 0.05, inclination 0.08726646 rad, longitude of the periapse 0.52359878 rad, right ascension of the ascending node 0.17453293 rad, and a final orbit with semi-major axis of 20000 km, eccentricity 0.06, inclination 0.17453293 rad, longitude of the periapse 0.78539816 rad, right ascension of the ascending node 0.34906585 rad. This maneuver shows that the method can be applied in transfers involving larger amplitudes. In this example we used as initial values l = 17500 km, α_1 = 0.78539816 rad, and α_2 = 1.04719755 rad.

The Figures show the behaviour of some orbital elements versus time spent in the maneuver, in seconds. Figures 9 and 15 show the behaviour of the semi-major axis of the transfer orbit, in km. Figures 10 and 16 show the behaviour of the eccentricity of the transfer orbit. Figures 11 and 17 show the transfer angle in degrees. Figures 12 and 18 show the behaviour of the inclination of the transfer orbit, in degrees. Figures 13 and 19 show the plane change angle resulted from the first and second impulses, in degrees. Figures 14 and 20 show the velocity increment V_1 and V_2, and the total velocity increment V in km/s. Figures 21 and 22 show the plane change angle generated by the

impulses for the second example in more detail. Figures 23 and 25 show de resultant of the plane change ($\gamma_1 + \gamma_2$), and Figures 24 and 26 show the total plane change ($|\gamma_1| + |\gamma_2|$) in degrees for the first and second example, respectively.

5- CONCLUSIONS

From Figures 9 to 26 and from other examples studied in Rocco [40], we can verify that, in a general way, when the maneuver spends less time the semi-major axis and the eccentricity of the transfer orbit increases, and when the maneuver spends more time the velocity increment decreases and the transfer angle increases. These behaviors occur because, when the maneuver is performed with less time, the transfer orbit approaches to a hyperbolic orbit, so the semi-major axis and eccentricity tend to increase. When the maneuver is performed with more time the transfer angle can be greater and the impulse directions approach the direction of the motion of the spacecraft. However, the impulse directions will never be in the direction of the motion, because there is always a component orthogonal to the orbital plane. This component provides a plane change, as shown in Figures 13 and 19. We can verify, in Figure 13, that, when the maneuver spends less time the plane change angle increases. In the second example, shown in Figure 19, this fact also occurs, as shown in more details in Figures 21, 22, 23 and 24. Figure 21 and 22 show the plane change angle resulted from the first and second impulse, respectively. In these figures, it is easy to verify that there is a small variation in the value of the plane change angle along the time. In Figure 21 we have a curve that initially decreases with the time, but around 2950 seconds the curve turns to increase. However, Figure 22 show that the value of the plane change angle resulted from the second impulse has a clear tendency to decrease with time. Therefore the resultant of the plane change, shown in Figure 23, and the total plane change angle, shown in Figure 24, decrease along the time. In the first example, although the resultant of the plane change increases along the time, as shown in Figure 25, the total plane change angle, shown in Figure 26, presents the same tendency of Figure 24, regarding the second example. The small increase in the value of the total plane change angle, observed in Figure 26, is due to a change of geometry of the maneuver that happens about 2600 seconds. Comparing these figures with Figures 14 and 20, it is possible to verify that, for a high plane change, there is a high value of the velocity increment. This is expected because changes in inclination, in general, spend more fuel. The increase in the plane change angle occur because when the fixed time is small, the spacecraft have to perform the maneuver very fast, then there is a great plane change in the first impulse and another great plane change in the second impulse. But the sum of the plane changes angles almost remains constant because the second impulse reverse part of the plane change angle resulted from the first impulse. But the resultant of the plane change is not equal to the difference among the inclinations of the initial and final orbits, because these orbits usually do not cross, because the maneuver does not correct just the difference in inclination, but also correct the eccentricity, the longitude of the periapside, the right ascension of the ascending node and the semi-major axis. Beyond this, we can verify that, for the first example, the semi-major axis and the eccentricity of the transfer orbit, shown in Figures 9 and 10, stabilized quickly. Therefore, inclination changes prevailed in the maneuver, thus most of the velocity increment applied in the maneuver is owed by the plane change. In the second example, the semi-major axis and the eccentricity, shown in Figures 15 and 16, present a high variation along the time without stabilizing around a specific value. In this way, the changes in the semi-major axis and in the eccentricity dominate the maneuver, prevailing with respect to inclination changes. But, in both examples, the behavior of the velocity increment is the same. The velocity increment decreases with time. However, there is a limit that occurs when the transfer angle is greater than 180°. After this limit, the increment velocity increases with time because, in this case, the impulse directions depart from the direction of the spacecraft motion. But, there is another kind of solutions that consider one or more complete revolutions in the transfer orbit before the injection into the final orbit, as foreseen in Equation 33. In this kind of solutions the time specified for the maneuver can be very high, in fact, this is recommended to cases when the time specified is greater than the period of the initial and final orbits.

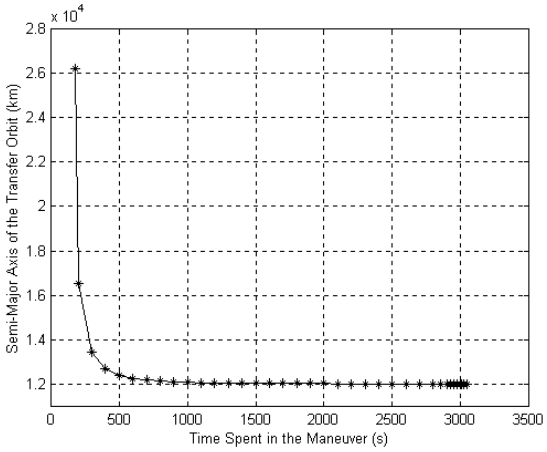

Fig. 9 – Semi-Major Axis vs. Time Spent in the Maneuver (1° example).

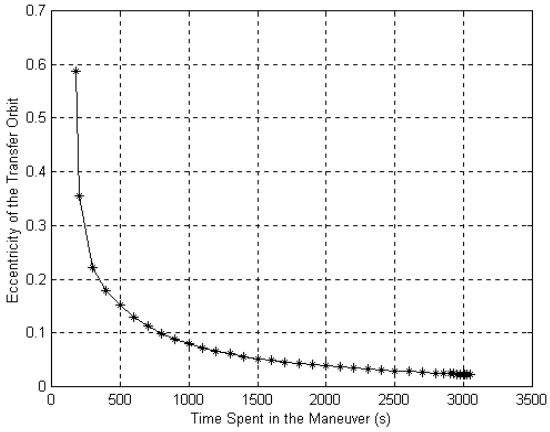

Fig. 10 – Eccentricity vs. Time Spent in the Maneuver (1° example).

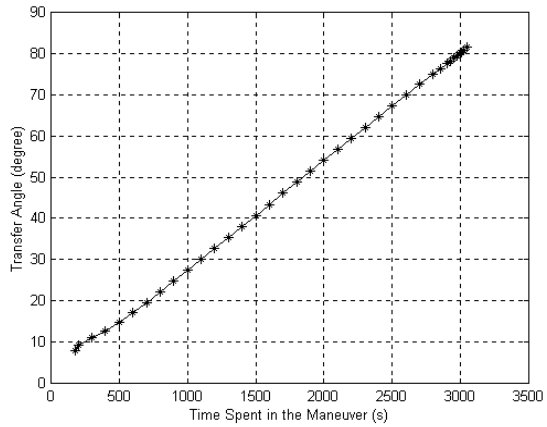

Fig. 11 – Transfer Angle vs. Time Spent in the Maneuver (1° example).

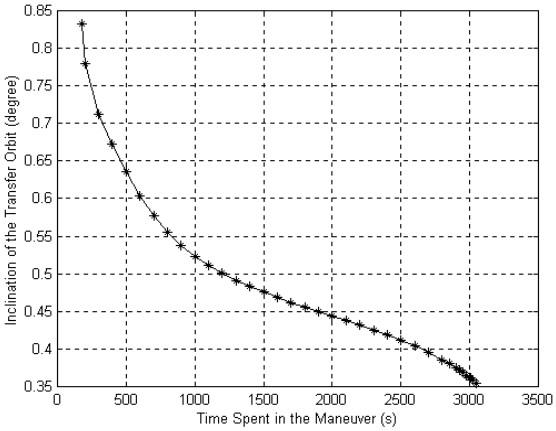

Fig. 12 – Inclination vs. Time Spent in the Maneuver (1° example).

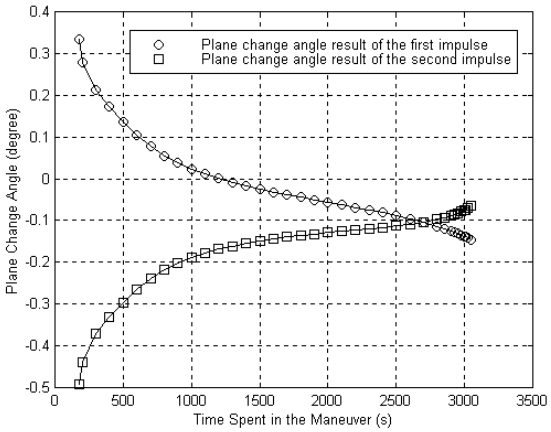

Fig. 13 – Plane Change Angle vs. Time Spent in the Maneuver (1° example).

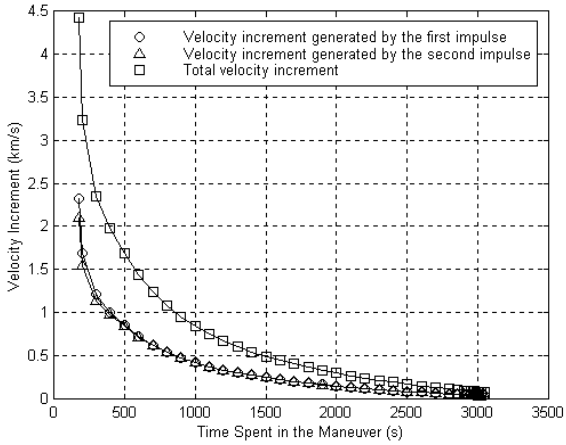

Fig. 14 – Velocity Increment vs. Time Spent in the Maneuver (1° example).

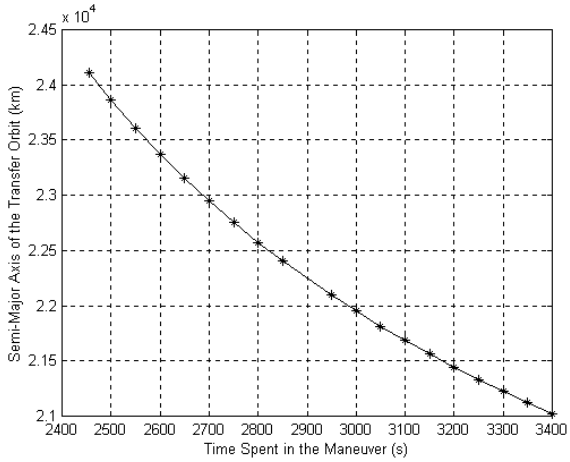

Fig. 15 – Semi-Major Axis vs. Time Spent in the Maneuver (2^o example).

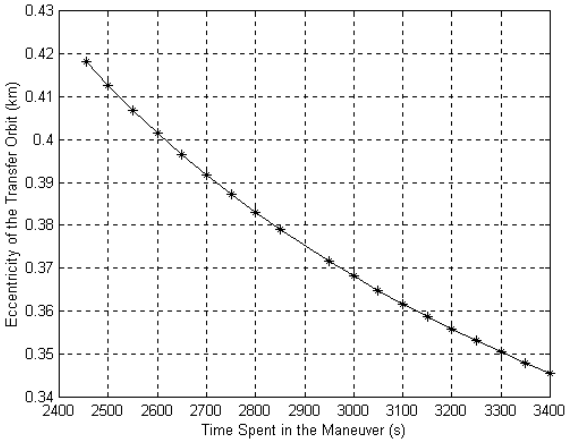

Fig. 16 – Eccentricity vs. Time Spent in the Maneuver (2^o example).

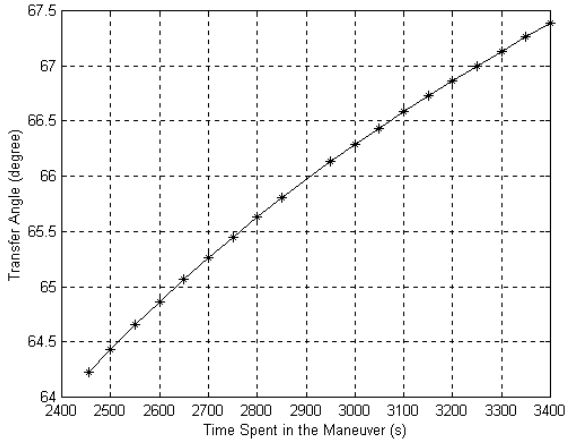

Fig. 17 – Transfer Angle vs. Time Spent in the Maneuver (2^o example).

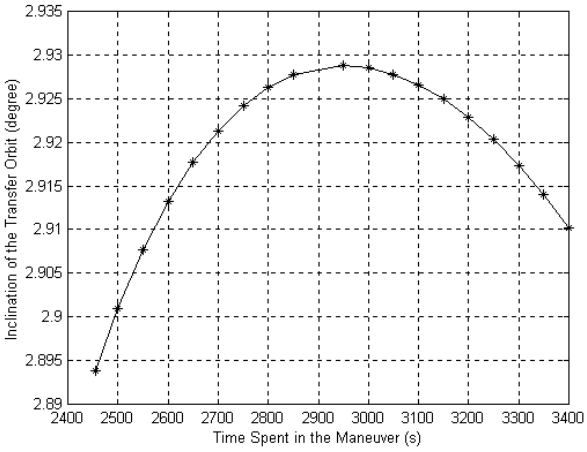

Fig. 18 – Inclination vs. Time Spent in the Maneuver (2^o example).

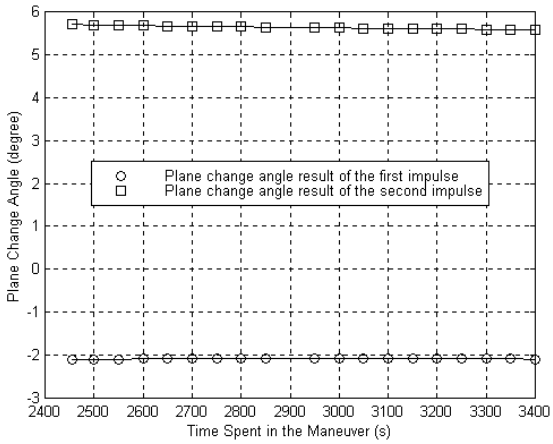

Fig. 19 – Plane Change Angle vs. Time Spent in the Maneuver (2^o example).

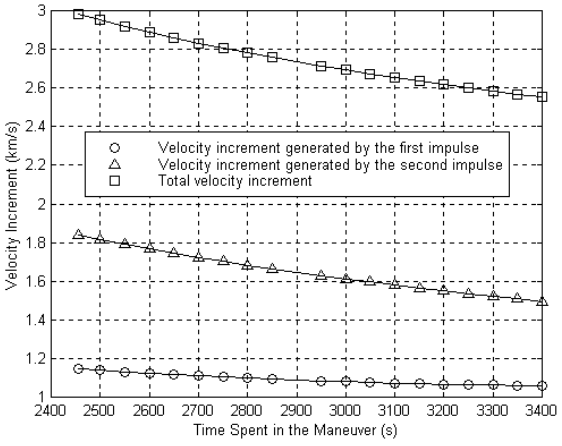

Fig. 20 – Velocity Increment vs. Time Spent in the Maneuver (2^o example).

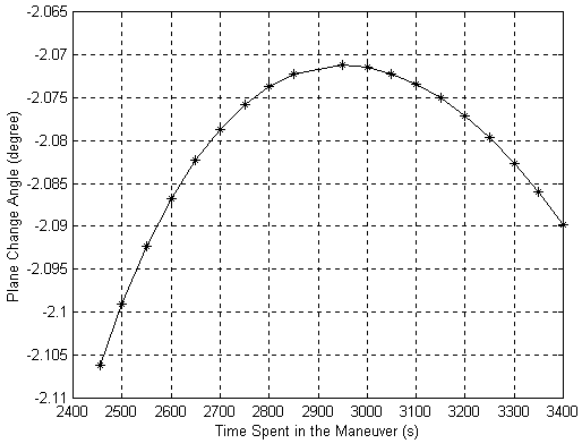

Fig. 21 – Plane Change Angle (γ_1) vs. Time Spent in the Maneuver (2^o example).

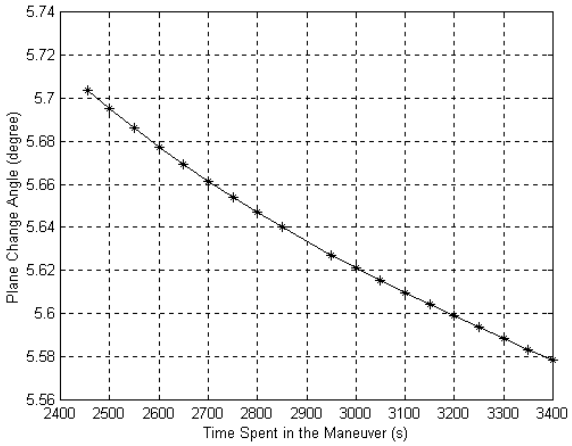

Fig. 22 – Plane Change Angle (γ_2) vs. Time Spent in the Maneuver (2^o example).

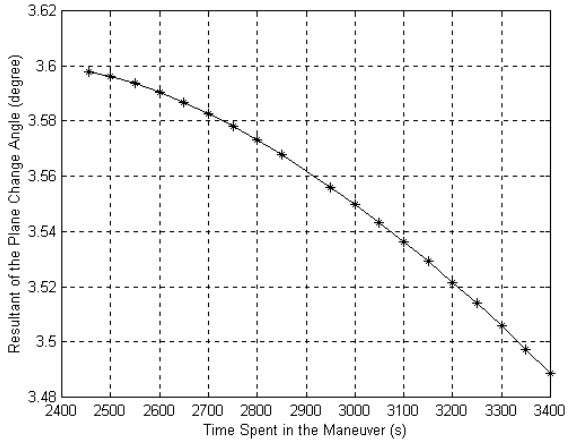

Fig. 23 – Resultant of the Plane Change vs. Time Spent in the Maneuver (2^o example).

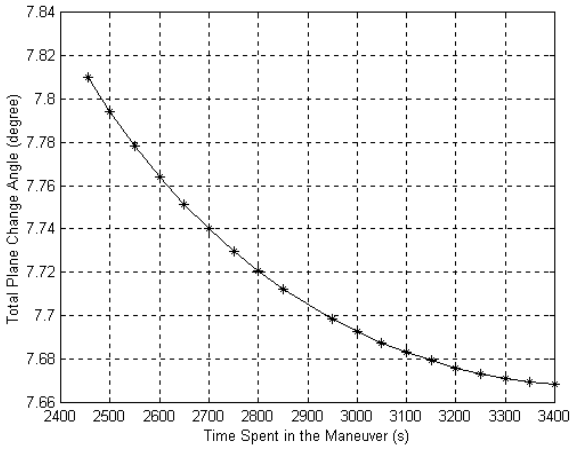

Fig. 24 – Total Plane Change Angle vs. Time Spent in the Maneuver (2^o example).

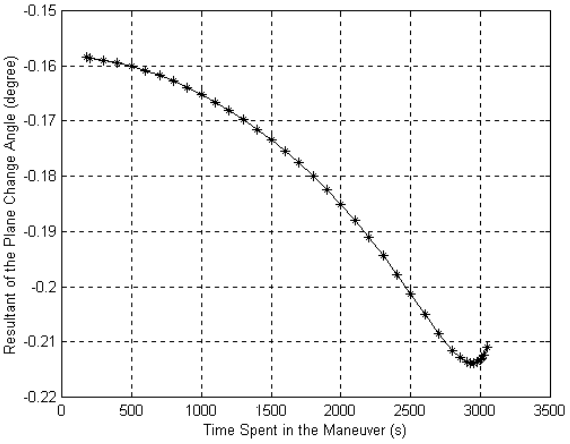

Fig. 25 – Resultant of the Plane Change vs. Time Spent in the Maneuver (1^o example).

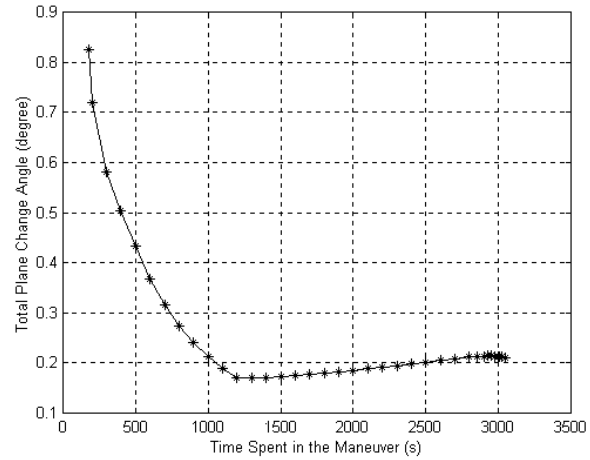

Fig. 26 – Total Plane Change Angle vs. Time Spent in the Maneuver (1^o example).

Besides that, we should advise that the software developed can not supply the solution for all combinations of the input parameters. For certain values of time, it can be impossible to obtain one solution because, for a very small or very large values of the time spent in the maneuver, the solution can not exist, or the numerical algorithms used in the software do not converge for

the solution, because the initial values used are too far from the solution. So, it is recommended a physical analysis of the problem, which takes into account the periods of the initial and final orbits, to find the range of values for the time spent in the maneuver, which is possible to accomplish the maneuver.

Another question to be solved is if the solution is a local or global minimum. Up to where we verified, the solution obtained seems to be a global minimum, because for the same input parameters, but using different initial values, it was not possible, to obtain better results. It is important to notice that the software tests automatically all the results, verifying if the maneuver obtained is just a mathematical solution or if it can really be implemented. When we use numerical methods there are some solutions, which satisfy the equations, however, in practice, they are impossible. Due to this fact, all the points shown in the graphs were tested and they represent solutions capable of being implemented. Thus, the developed software was tested with success.

Acknowledgements

The authors express their thanks to the National Council for Scientific and Technological Development in Brazil (CNPq) and the Foundation for Supporting Research in São Paulo State (FAPESP), for supporting this research.

References:

[1] Lawden, D.F., Minimal Rocket Trajectories. *ARS Journal*, Vol. 23, n. 6, 1953, pp. 360-382.

[2] Lawden, D.F., Fundamentals of Space Navigation. *JBIS*, Vol. 13, 1954, pp. 87-101.

[3] Zee, C.H., Effect of finite thrusting time in orbital maneuvers. *AIAA Journal*, Vol. 1, n. 1, 1963, pp. 60-64.

[4] Pierson, B.L. and Kluever, C.A., Three-stage approach to optimal low-thrust Earth-moon trajectories . *Journal of Guidance, Control, and Dynamics*, Vol.17, n.6, 1994, pp. 1275-1282.

[5] Casalino, L.; Colasurdo, G., and Pasttrone, D., Optimal Low-Thrust Scape Trajectories Using Gravity Assist. *Journal Of Guidance, Control and Dynamics,* Vol. 22, n. 5, 1999, pp. 637-642.

[6] Sukhanov A.A. and Prado A.F.B.A., Constant tangential low-thrust trajectories near an oblate planet", *Journal of Guidance Control and Dynamics*, Vol. 24, n. 4, 2001, pp. 723-731.

[7] Betts, J.T. and Erb, S.O., Optimal low thrust trajectories to the Moon**.** *SIAM Journal on Applied Dynamical Systems*; Vol. 2, n. 2, 2003, pp**.** 144-171.

[8] Santos, D.P.S.; Prado, A.F.B.A; Casalino, L. and Colasurdo, G., Optimal trajectories towards near-earth-objects using solar electric propulsion (sep) and gravity assisted maneuver. *Journal of Aerospace Engineering, Sciences and Applications*, Vol. I, n. 2, 2008, pp.51-64. (http://www.aeroespacial.org.br/jaesa/editions/repository/v01/n02/6-SantosEtal.pdf)

[9] Prado, A.F.B.A., Low-Thrust Trajectories to the Moon. In: Nikos Mastorakis. (Org.). Computer and Simulation in Modern Science. Sofia: WSEAS Press, 2008, Vol. 1, pp. 89-94.

[10] Gomes, V.M.; Prado, A.F.B.A. and Kuga, H.K., Low thrust maneuvers for artificial satellites. *WSEAS Transactions on Applied and Theoretical Mechanics*, Vol. 03, 2008, pp. 1-10.

[11] Song, Y.J.; Park, S.Y.; Choi, K.H. and Sim, E.S., A lunar cargo mission design strategy using variable low thrust. *Advances in Space Research*, Vol.43, n. 9, 2009, pp.1391-1406.

[12] Fazelzadeh, S.A. and Varzandian, G.A., Minimum-time Earth–Moon and Moon–Earth orbital maneuvers using time-domain finite element method. *Acta Astronautica*, Vol. 66, n. 3, 2010, pp.528-538.

[13] Gomes, V.M. and Prado, A.F.B.A., Avoiding collisions maneuvers using a stochastic approach. *WSEAS International Journal of Mechanics*, Vol. 5, 2011, pp. 148-156.

[14] Santos, D.P.S. and Prado, A.F.B.A. Optimal Low-Thrust Trajectories to Reach the Asteroid Apophis. *WSEAS Transactions on Applied and Theoretical Mechanics*, Vol. 7, 2012, pp. 241-251.

[15] Santos, D.P.S.; Casalino, L.;Colasurdo, G. and Prado, A.F.B.A,. Optimal Trajectories towards Near-Earth-Objects using Solar Electric Propulsion (SEP) and Gravity Assisted Maneuver. *WSEAS Transactions on Applied and Theoretical Mechanics*, Vol. 4, 2009, pp. 125-135.

[16] Hohmann, W., Die Erreichbarkeit der Himmelskorper. Oldenbourg, Munique, 1925.

[17] Hoelker, R.F. and Silber, R., The Bi-Elliptic Transfer Between Circular Co-Planar Orbits. Tech Memo 2-59, Army Ballistic Missile Agency, Redstone Arsenal, Alabama, USA, 1959.

[18] Shternfeld, A., Soviet Space Science, Basic Books, Inc., New York, 1959, pp. 109-111.
[19] Ting, L., Optimum orbital transfer by several impulses. *Astronautical Acta*, Vol. 6, n. 5, 1960, pp. 256-265.
[20] Bender, D.F., Optimum coplanar two-impulse transfers between elliptic orbits. *Aerospace Engineering*, 1962, pp. 44-52.
[21] Eckel, K.G., Optimum transfer in a central force field with n impulses. *Astronautica Acta*, Vol. 9, n. 5/6, 1963, pp. 302-324.
[22] Wang, K., Minimum Time Transfer Between Coplanar Circular Orbits by Two Impulses and Propulsion Requirements. *Astronautica Acta,* Vol. 9, n. 1, 1963, pp. 12-19.
[23] McCue, G.A. and Bender, D.F., Numerical Investigation of Minimum Impulse Orbital Transfer. *AIAA Journal,* Vol. 3, n. 12, 1965, pp. 2328-2333.
[24] Roth, H.L., Minimization of the velocity increment for a bi-elliptic transfer with plane change. *Astronautical Acta*, Vol. 13, n. 2, 1967, pp. 119-130.
[25] Jezewski, D.J. and Rozendaal, H.L., An efficient method for calculating optimal free-space N-impulsive trajectories. *AIAA Journal*, Vol. 6, n. 11, 1968, pp. 2160-2165.
[26] Lion, P.M. and Handelsman, M., Primer vector on fixed-time impulsive trajectories. *AIAA Journal*, Vol. 6, n. 1, 1968, pp. 127-132.
[27] Prussing, J.E., Optimal four-impulse fixed-time rendezvous in the vicinity of a circular orbit. *AIAA Journal*, Vol. 7, n. 5, 1969, pp. 928-935.
[28] Prussing, J.E., Optimal two- and three-impulse fixed-time rendezvous in the vicinity of a circular orbit. *AIAA Journal*, Vol. 8, n. 7, 1970, pp. 1221-1228.
[29] Gross, L.R. and Prussing, J.E., Optimal multiple-impulse direct ascent fixed-time rendezvous. *AIAA Journal*, Vol. 12, n. 7, 1974, pp. 885-889.
[30] Walton, J. M.; Marchal, C. and Culp, R.D., Synthesis of the Types of Optimal Transfers between Hyperbolic Asymptotes, *AIAA Journal*, Vol.13, n. 8, 1975, pp. 980-988.
[31] Ivashkin, V.V. and Skorokhodov, A.P., Definition and Analysis of Properties of Optimal Three-Impulse Point-to-Orbit Transfers Under Time Constraint. *Acta Astronautica,,* Vol. 8, n. 1, 1981, pp. 11-23.
[32] Eckel, K.G., Optimal impulsive transfer with time constraint. *Astronautica Acta*, Vol. 9, n. 3, 1982, pp. 139-146.
[33] Eckel, K.G. and Vinh, N.X., Optimal Swtitching Conditions for Minimum Fuel Fixed Time Transfer Between non Coplanar Elliptical Orbits. *Acta Astronautica,* Vol. 11, n. 10/11, 1984, pp. 621-631.
[34] Prussing, J.E. and Chiu, J.H., Optimal multiple-impulse time-fixed rendezvous between circular orbits. *Journal of Guidance, Control, and Dynamics*, Vol. 9, n. 1, 1986, pp. 17-22.
[35] Jin, H. and Melton, R.G., Transfers between circular orbits using fixed impulses. AAS paper 91-161. In: AAS/AIAA Spaceflight Mechanics Meeting, Houston, TX, 11-13 Feb. 1991.
[36] Prado A.F.B.A. and Broucke, R.A., Transfer Orbits in Restricted Problem, *Journal of Guidance Control and Dynamics*, Vol. 18, n. 3, 1995, pp. 593-598.
[37] Taur, D.R.; Carroll, V.C. and Prussing, J.E., Optimal Impulsive Time-Fixed Orbital Rendezvous and Interception with Path Constraints. *Journal of Guidance, Control, and Dynamics,* Vol. 18, n. 1, 1995, pp. 54-60.
[38] Prado, A.F.B.A. and Broucke, R.A., Transfer orbits in the Earth-Moon system using a regularized model. *Journal of Guidance, Control and Dyn*amics, Vol. 19, n.4, 1996, pp.929-933.
[39] Prado, A.F.B.A., Travelling between the Lagrangian points and the Earth, *Acta Astronautica,* Vol. 39, n. 7, 1996, pp. 483-486.
[40] Rocco, E.M., *Transferências Orbitais Bi-Impulsivas com Limite de Tempo.* Master Thesis, (INPE-6676-TDI/626, 1997.
[41] Rocco, E.M.; Prado, A.F.B.A. and Souza, M.L.O., *Bi-Impulsive Orbital Transfers Between Non-Coplanar Orbits with Time Limit*. Sixth Pan American Congress of Applied Mechanics PACAM VI / 8th International Conference on Dynamic Problems in Mechanics DINAME. Rio de Janeiro - RJ, 1999.
[42] Rocco, E.M.; Prado, A.F.B.A.; Souza, M.L.O. and Baldo, J.E., Optimal bi-impulsive non-coplanar maneuvers using hyperbolic orbital transfer with time constraint. *Journal of Aerospace Engineering, Sciences and Applications*, Vol. I, n. 2, 2008, pp. 43-50.
[43] Press, W.H.; Teukolsky, S.A.; Vetterling, W.T. and Flannery, B.P., *Numerical Recipes in FORTRAN (The Art of Scientific Computing)*, 2nd Ed. Cambridge University Press, 1992.